

Robustness of observation-based decadal sea-level variability in the Indo-Pacific Ocean

A. G. Nidheesh^{1,3}, M. Lengaigne^{1,2}, J. Vialard¹, T. Izumo^{1,2}, A.S. Unnikrishnan³,
B. Meyssignac⁴, B. Hamlington⁵, C. de Boyer Montegut⁶

¹*LOCEAN-IPSL, Sorbonne Univ. (UPMC, Univ Paris 06)-CNRS-IRD-MNHN, Paris, France*

²*Indo-French Cell for Water Sciences, IISc-NIO-IITM-IRD Joint International Laboratory, CSIR-NIO, Goa, India*

³*CSIR-National Institute of Oceanography, Goa, India*

⁴*LEGOS, CNES, CNRS, IRD, UPS, Université de Toulouse, Toulouse, France*

⁵*Old Dominion University, Department of Ocean, Earth and Atmospheric Sciences, Norfolk, VA, USA*

⁶*Laboratoire d'Océanographie Physique et Spatiale, UBO/Ifremer/CNRS/IRD, Brest, France*
to be submitted to *Geophysical Research Letters*

Corresponding author address:

A. G. Nidheesh
LOCEAN-IPSL, Sorbonne Universités
Paris, France
E-mail: gnidheesh@locean-ipsl.upmc.fr

Abstract

We examine the consistency of Indo-Pacific decadal sea-level variability in ten gridded, observation-based sea-level products for the 1960-2010 period. Decadal sea-level variations are robust in the Pacific, with more than 50% of variance explained by decadal modulation of two flavors of El Niño Southern Oscillation (classical ENSO and Modoki). Amplitude of decadal sea-level variability is weaker in the Indian Ocean than in the Pacific. All datasets indicate a transmission of decadal sea-level signals from the western Pacific to the northwest Australian coast through the Indonesian throughflow. The southern tropical Indian Ocean sea-level variability is associated with decadal modulations of ENSO in reconstructions but not in reanalyses or *in-situ* dataset. The Pacific-independent Indian Ocean decadal sea-level variability is not robust, but tends to be maximum in the southwestern tropical Indian Ocean. The inconsistency of Indian Ocean decadal variability across the sea-level products calls for caution in making definitive conclusions on decadal sea-level variability in this basin.

Index terms: 4556; 4522; 4513

Keywords: Decadal variability, sea-level, IO, climate

Key points:

1. Pacific Ocean decadal sea-level variability is robust and largely driven by decadal modulation of ENSO and Modoki
2. Indian Ocean decadal sea-level variability (either related to or independent from the Pacific) is inconsistent across observation-based sea-level products

Introduction

Identifying, understanding and projecting sea-level changes is of critical importance for assessing its socio-economic and environmental impacts and for planning and adaptation strategies. This is particularly true for the tropical Indo-Pacific region, which hosts a large number of highly populated low-lying coastal zones. China, India, Bangladesh, Vietnam and Indonesia are for instance the top 5 countries for population at risk from sea-level rise, with more than 350 million people involved [Neumann *et al.*, 2015]. While the global mean sea level (GMSL) has been rising consistently at a rate of about 3.3 mm yr^{-1} over the last two decades [e.g. Fasullo *et al.*, 2016], regional sea-level changes can deviate considerably from this global mean rate, to the point that local and global trends can differ in sign at some locations [Stammer *et al.*, 2013]. This spatially non-uniform pattern in regional sea-level trends mainly arises from changes in surface wind patterns in response to both natural climate variability (especially at decadal/multi-decadal timescales) and anthropogenic climate change [Stammer *et al.*, 2013]. Identifying the sea-level imprint of natural climate variability, especially at decadal timescales, is hence crucial for separating the effects of natural climate variability and anthropogenic forcing on observed sea-level change.

The El Niño Southern Oscillation (ENSO) is the leading mode of interannual climate variability, and involves large sea-level signals in the tropical Pacific [e.g. Widlansky *et al.*, 2015]. The Interdecadal Pacific Oscillation (IPO), for which the decadal ENSO modulation is an active driver [Power *et al.*, 1999, Newman *et al.*, 2016], is a major partaker of low-frequency sea-level variations in the Pacific Ocean [e.g. Bromirski *et al.*, 2011; Meyssignac *et al.*, 2012b; Hamlington *et al.*, 2013; Frankcombe *et al.*, 2015; Palanisamy *et al.*, 2015], inducing opposite sea-level decadal signals in the western tropical Pacific and central/eastern equatorial Pacific. These decadal variations strongly contribute to regional sea-level trends over the past two decades, including the accelerated (reduced) rise relative to the global rate in the western (eastern) tropical Pacific [e.g. Merrifield 2011; Zhang and Church, 2012; Moon *et al.*, 2013; Frankcombe *et al.*, 2015; Hamlington *et al.*, 2014]. El Niño events come in two primary “flavors”, with maximum surface temperature and sea-level anomalies (SLA) occurring either in the east or central Pacific. Central Pacific El Niños have been nicknamed Modoki events [Ashok *et al.*, 2007]. The decadal modulation of Modoki events is associated with decadal sea-level variation in the northern Pacific, referred to as the North Pacific Gyre Oscillation [Di Lorenzo *et al.*, 2010]. Behera and Yamagata [2010; hereafter BY2010] also suggested, based on a 8-years satellite altimetry record analysis, that central Pacific decadal sea-level variations are strongly related to Modoki decadal modulation.

While decadal climate variability and its sea-level imprint are rather well documented in the

Pacific, this is not the case in the Indian Ocean (IO hereafter), primarily because of the scarcity of long-term observations in this basin [e.g. *Han et al.*, 2014]. There is a well established oceanic bridge at inter annual [e.g. *Feng et al.* 2003] and decadal timescales between the western equatorial Pacific and southeast IO [*Feng et al.*, 2004, 2010; *Trenary and Han*, 2013; *Schwarzkopf and Boning*, 2011; *Nidheesh et al.*, 2013 (hereafter N2013)], via the coastal wave-guide in the Indonesian through flow region (in the following, we always refer to the connection between the Pacific and IO via the Indonesian Through flow as the “oceanic bridge”). Apart from this oceanic bridge, there is no consensus on how the Pacific influences IO decadal sea-level variability through atmospheric teleconnections. Based on the short 1993-2006 altimeter record, *Lee and McPhaden* [2008] suggested that the IPO is associated with southern tropical IO decadal sea-level variations through atmospheric teleconnections. However, using an ocean model simulation, *N2013* showed that this apparent IPO control on IO decadal sea-level variability breaks down over the longer period of 1966-2007. Along the same lines, the respective influence of remote and local wind forcing on decadal sea-level variations in the southern tropical IO appears to vary considerably depending on the period and dataset [e.g. *Schwarzkopf and Boning*, 2011; *Trenary and Han*, 2013; *Zhuang et al.*, 2013; *N2013*; *Li and Han*, 2015]. Recent studies suggest that the main cause of the recent ‘hiatus’ in global surface warming is associated with an increase in the heat uptake by the Pacific during a negative IPO phase and that excess heat was largely transferred to the IO through the oceanic bridge [*Lee et al.*, 2015; *Nieves et al.*, 2016]. This is a striking example of how natural decadal climate variability obscures the anthropogenic climate change, and a strong incentive to better understand IO decadal sea-level (and heat content) variations and their linkage to the Pacific decadal variability.

The study of Indo-Pacific decadal sea-level variability requires gridded datasets that span several decades. The modern satellite altimetry offers sea-level measurements with a near-global coverage but only spans 24 years. On the other hand, tide gauge sea-level measurements are confined to coastal regions and islands, preventing a thorough assessment of open ocean variability. The lack of long-term, near-global sea-level data hence prompted the scientific community to develop a number of different gridded sea-level datasets, providing global sea-level estimates for at least the past fifty years. This includes *reconstructions* [e.g. *Church et al.* 2004; *Church and White*, 2011; *Hamlington et al.*, 2011; *Meyssignac et al.*, 2012a] that combine spatial patterns derived from the altimetry or ocean models with longer time series from tide gauge records to estimate sea level over multi-decadal epochs. *N2013* showed that steric sea-level variations in the tropical Indo-Pacific are primarily driven by thermal variations in the upper thousand meters. Hence the historical *in-situ* subsurface temperature data – largely a few XBT lines – can be interpolated in space to estimate

thermohaline sea-level changes [e.g. *Levitus et al.*, 2012] or built into an ocean *reanalysis* to simulate sea level over the historical period. Caveats for those products (reconstructions and reanalyses) include sparse observational coverage, assumptions in the interpolation method, model errors and errors in decadal wind fluctuation estimates [e.g. N2013]. This can lead to significant biases in the representation of sea-level variability in those observation-based data.

To our knowledge, there is currently no thorough evaluation of the consistency of Indo-Pacific decadal sea-level variations among available products. In the present paper, we examine ten gridded sea-level products available for the period of 1960-2010 (three reanalyses, six reconstructions, one *in-situ* based product) to address the following questions. Are the dominant patterns of Pacific decadal sea-level variability identified in earlier studies robust across these different gridded sea-level datasets? Is the sea-level imprint of the Pacific decadal climate variability robust over the IO? Is there any robust Pacific-independent decadal sea-level variability in the IO?

2. Data and methods

We use ten gridded sea-level products available over their overlapping period of 1960-2010 to investigate if they display coherent decadal sea-level variability over the Indo-Pacific region. A general description of the products is given below, but a more thorough description of each product is provided in the supplementary material. We used thermohaline sea level computed from the World Ocean Data (hereafter WO) [*Levitus et al.*, 2012 for details]. We also used three ocean reanalyses: ORA-S4 (Ocean Reanalysis System 4 from the European Centre for Medium-Range Weather Forecasts (ECMWF); hereafter OR) [*Balmaseda et al.*, 2013], SODA2.2.4 (Simple Ocean Data Assimilation; hereafter SO) [*Carton and Giese*, 2008] and GECCO (German contribution to the consortium for Estimating the Circulation and Climate of the Ocean; hereafter GE) [*Köhl and Stammer*, 2008]. We further considered 6 different sea-level reconstructions. Three of them are based on altimetry-derived basis functions [*Church and White*, 2011 (CW); *Hamlington et al.*, 2011; 2012 (HA); *Meyssignac et al.*, 2012a (M1)]. Since sea-level reconstructions are sensitive to the dataset from which the basis functions are derived [see *Meyssignac et al.*, 2012a], we also used three additional reconstructions similar to *Meyssignac et al.* [2012a], but whose basis functions are derived from the three ocean reanalyses mentioned above (i.e. OR (M2), SO (M3) and GE (M4)).

All the above datasets have a monthly resolution. We interpolated each dataset to a regular $2.5^\circ \times 2.5^\circ$ grid. Interannual and decadal (defined as the variability above 7 year periodicity) components of variability are extracted using the seasonal-trend decomposition procedure described in *Cleveland et al.* [1990]. Some of the products we use (WO & reanalyses) do not account for the

spatially uniform sea-level rise due to changes in ocean mass (while reconstructions do). Since this study focuses on regional sea-level variability, the globally-averaged sea-level time series (Fig. S1) is subtracted from each grid-point for all datasets.

The indices of the leading decadal climate modes in the tropical Pacific (classical ENSO and Modoki decadal variations) are defined through an Empirical Orthogonal Function (EOF) analysis of HadISST [Rayner *et al.*, 2003], a typical method of climate mode indices definition used in previous studies [e.g. Newman *et al.*, 2003; Nidheesh *et al.*, 2017]. These time series are strongly correlated with the decadal-filtered classical ENSO and Modoki indices (0.97 and 0.76 correlation respectively, Fig. S2), and similar results were obtained when using those classical indices (not shown).

We consider the ensemble mean as an indicator of consensus variability in the 10 sea-level products. To assess the inter-product consistency, we computed the inter-product *spread* as the square root of the mean squared deviations from the ensemble mean, averaged over products and time. We then defined a metric called the *agreement ratio* as the *spread* divided by the standard deviation of the ensemble mean variability. This *agreement ratio* is used as a metric that summarizes the spread in variability between the products relative to the mean amplitude of the variability (computational details of agreement ratio are given in the supplementary information).

3. Results

Fig. 1a displays the standard deviation of ensemble-mean (for the ten products) decadal sea-level variability in the Indo-Pacific region. Strongest decadal sea-level variations (2 to 3 cm) occur in the western tropical Pacific, as well as east of Japan in the Kuroshio extension region. Weaker decadal sea-level variability, relative maxima (~1 cm), occurs along the west coast of America and in the central Pacific mid-latitudes of both hemispheres (around 30°). In general, the amplitude of IO decadal sea-level variability is weaker than Pacific variability, with largest signals along the western Australian coast (~2 cm), in the southern tropical IO (~1.5 cm), in the eastern equatorial IO and along the rim of Bay of Bengal (BoB, ~1 cm). Similar regions of maximum decadal variability are found in the shorter altimetry data (see Fig. S3).

The white (respectively black) stippling on Fig. 1a indicates grid-points where the “agreement ratio” defined in Section 2 is less than 0.5 (resp. 1), i.e. where the disagreement between products is small compared to the sea-level ensemble-mean decadal variability. In the Pacific, regions of large decadal sea-level variations are generally consistent amongst products, except in the Kuroshio extension region (decadal variability in this region is largely due to oceanic intrinsic variability

[Serazin *et al.*, 2015] which is not the same in different models and very difficult to tame to observations even when assimilating data). This agreement is particularly strong (white stippling) in the western and eastern tropical Pacific. The picture is very different in the IO where the analyzed products exhibit inconsistent decadal sea-level variations in most of the regions. A large area of moderate inter-product agreement (black stippling) is however found along the west coast of Australia. Sparse black stippling indicates a modest inter-product agreement in the southern tropical IO. In contrast, decadal sea-level variations in the eastern equatorial IO and in the BoB are not consistent amongst the products. Fig. 1b displays the zonal distribution of the *agreement ratio* averaged over 20°S-20°N in the Indo-Pacific region. While this ratio is nearly 0.5 in the western and eastern tropical Pacific and 1 in the central tropical Pacific, it ranges from 1 to 2 in the tropical IO west of 110°E. This simple diagnostic clearly illustrates the larger inter-products spread in the tropical IO than in the tropical Pacific, except along the west Australian coast.

Figures 2a,d display the ensemble average patterns of the first two EOFs of decadal sea-level variability, performed over the Pacific domain [120°E-70°W, 45°S-60°N] for the 1960-2010 period. These first two EOFs collectively explain more than 50% (Figs. S4,S5) of Pacific decadal sea-level variance for all products (70% on average, see Fig. 2). The first EOF pattern (Fig. 2a, ~ 54% of variance on average) in the Pacific is reminiscent of the sea-level signature of the positive IPO phase [e.g. Meyssignac *et al.* 2012a; Hamlington *et al.* 2013]. This is confirmed by the strong correlation of the corresponding ensemble mean principal component (PC) with the decadal ENSO index ($r=0.94$, Fig. 2b), with a very small inter-products spread (correlation above 0.8 for all products except GE; see Fig. S4). The abnormally weak trade winds during the decadal ENSO positive phase (fig. S2) induce a large-scale sea-level seesaw in the tropical Pacific, with positive anomalies in the central/eastern and negative anomalies in the western tropical Pacific. The positive SLA in the eastern Pacific propagate poleward along the American coast as coastal Kelvin waves and westward into the basin as Rossby waves, with faster Rossby wave propagation at low latitudes explaining the V-shaped pattern with larger offshore extent in the tropics [e.g. N2013]. This mode also exhibits a negative sea-level signature in the central Pacific mid-latitudes of both hemispheres (around 30°), via atmospheric teleconnections between the tropical Pacific and surface wind-stress curl in the mid-latitude low-pressure regions [e.g. Moon *et al.* 2013]. A narrow negative sea-level signal is also evident off the Japanese coast in the Kuroshio extension region. As in Fig. 1, stippling indicates regions of low agreement ratio (a good inter-products agreement), but here for the decadal sea-level signal projected on that EOF. This stippling indicates that the sea-level signal associated with decadal ENSO is very robust in the regions discussed above (see also individual patterns on Fig. S4).

The pattern correlation between individual EOFs and the ensemble mean EOF exceeds 0.8 for all products except GE (0.65), highlighting the robustness of this EOF pattern in the Pacific across the products (Fig. 2c).

The second EOF of decadal sea level in the Pacific (Fig. 2d, ~ 18% of variance on average) is characterized by a broad positive SLA in the western-central tropical Pacific (~15°S to ~5°N) and a narrow band of positive SLA off the east coast of Japan. Negative SLA are evident in the northwest tropical Pacific (southeast of Philippines) and along the west coast of tropical south America (Fig. 2d). This pattern is reminiscent of the one described as the imprint of decadal Modoki variability in BY2010. The 0.81 correlation between the corresponding ensemble PC and the decadal Modoki index (Fig. 2e) further confirms that this pattern is associated with decadal modulation of Modoki. The inter-product consistency for this second mode is however weaker than that of the first EOF (no white stippling), with an inter-products agreement mostly in the central and western tropical Pacific (stippling on Fig. 2d; see also individual patterns on Fig. S5). Individual EOF2 patterns are also less consistent with the ensemble mean pattern for the Pacific, with lower pattern correlations, ranging from 0.4 to 0.8 (Fig. 2f). The spread of the second PCs is also larger than that of the first PCs (Fig. 2b,e), especially before 1980, with correlations for individual products ranging from 0.4 to 0.85 (Fig. S5).

In the rest of the paper, we will refer to EOFs 1 and 2 on figure 2 as decadal ENSO and decadal Modoki, respectively. Note, we do not imply that decadal variations in the tropical Pacific are the sole drivers of, e.g. IPO variability, for which stochastic atmospheric forcing at mid latitudes, for instance, also matters [e.g. *Newman et al.* 2016]. However, recent experiments with coupled models indicate that specifying SST anomalies in the central and eastern equatorial Pacific allows reproducing global patterns of decadal variability, including in the IO [e.g. *Kosaka and Xie* 2013; *Dong et al.* 2015]. This is a strong indication that equatorial Pacific decadal SST variations associated with ENSO and Modoki are the common forcing source that establishes the global patterns associated with Pacific decadal climate variability.

These dominant modes in Pacific decadal sea-level variability are associated with signals in the IO. While the oceanic bridge associated with decadal ENSO fluctuations [e.g. *Feng et al.*, 2010] is robust across products, that associated with Modoki (BY2010) is more variable. The sea-level signal in the southern tropical IO, attributed by *Lee and McPhaden* [2008] to a remote control of the wind stress curl in this region (Fig. S2) through atmospheric teleconnections from the Pacific, appears in association with both decadal ENSO and Modoki, although the signal is consistent (but with sparse stippling) across the products only for ENSO (see stippling on Fig. 2a,d). The weak negative sea-

level imprint of both modes in the eastern equatorial IO and along the rim of BoB is not robust (Fig. 2a,d). The stippling on Fig. 2a,d in fact indicates that the sea-level signature of decadal ENSO and Modoki is more variable in the IO than in the Pacific. The IO sea-level pattern related to ENSO is quite variable from one product to another (pattern correlations from 0.4 to 0.8, Fig. 2c). These inter-products differences are even larger for IO decadal Modoki signals (pattern correlations from 0.1 to 0.8: HA and CW are outliers, being the only two products that do not indicate a decadal Modoki signature in the southern tropical IO: Fig. S5). Overall, decadal ENSO and Modoki sea-level signatures have varying amplitudes but always a consistent sign in key regions of the Pacific but have a larger spread that even changes sign in the IO (Fig. S6).

The above analyses show that, although variable amongst products, both decadal ENSO and Modoki have a remote influence on decadal sea-level variations in the IO. Fig. 3a further shows the percentage of IO decadal sea-level variance explained by these Pacific climate modes. The Pacific influence is systematically larger in reconstructions (~40% on average up to 80% in CW) as compared to other products (~20% average), most likely because the EOF truncation used in reconstructions yields minimum small-scale variability than in re-analyses or *in-situ* data. Fig. 3a hence illustrates that for all products except CW, 50 to 80% of the IO decadal sea-level variance is independent from the two leading modes of Pacific decadal variability. This calls for a specific assessment of the consistency of Pacific-independent IO decadal sea-level variability amongst different products. To that end, we estimated the Pacific-independent IO decadal sea-level variability by subtracting signals linearly related to decadal ENSO and Modoki indices (which are orthogonal by our definition based on EOFs) from the IO decadal sea-level signal. Fig. 3b displays the standard deviation of this ensemble mean Pacific-independent sea-level signal in the IO. Largest signals are found in a broad region in the southwestern tropical and subtropical IO, between 5°S-30°S, which partly overlaps the region where Pacific climate modes imprint their sea-level signatures (see Fig. 2a,d). There is however no consensus on this Pacific-independent variability depicted by each product (as revealed by very scarce stippling on Fig. 3bandvarying individual patterns on Fig. S7). While most products suggest a large Pacific-independent decadal sea-level variability in the IO, this variability is thus not consistent across the products.

Some of the diagnostics above suggest a different behavior from sea-level reconstructions relative to reanalyses and WO. First, the percentage of IO decadal sea-level variance explained by decadal ENSO and Modoki fluctuations is notably higher in reconstructions (on average 48%) than reanalyses and WO (23%, Fig. 3a). Second, the IO decadal ENSO pattern also tends to be different for reanalyses and WO than for reconstructions (red bars in Fig. 2c). We hence display the ensemble

average patterns of IO sea-level signature associated to decadal ENSO separately for reconstructions and rest of the products in Fig. 4b,c. The signal transmitted via the oceanic bridge to the west coast of Australia is consistent across all the products at both interannual and decadal timescales (Fig. 4a-c). On the other hand, the sea-level signature associated to atmospheric teleconnection between the Pacific and southern tropical IO, suggested by *Lee and McPhaden* [2008] is hardly visible in reanalyses and WO (Fig. 4c). In reconstructions, the IO decadal ENSO sea-level signature (Fig. 4b) largely resembles that of interannual ENSO (Fig. 4a), which itself is very similar to the IO Dipole (IOD) signature [e.g. *Webster et al.*, 1999] (there is a tendency for El Niño events to trigger positive IODs [e.g. *Annamalai et al.*, 2003]). High pattern correlation between IO interannual and decadal ENSO sea-level signatures in reconstructions (>0.8), compared to reanalyses and WOD (0.3 to 0.6; Fig. 4d) confirms the similarity of interannual and decadal ENSO sea-level signatures in reconstructions. One plausible reason for this similarity is linked to the sea-level reconstruction methodology, which projects the leading EOFs of global sea level over a long period using the tide gauge records. While the distribution of tide gauges is sufficiently dense to constrain the spatial pattern of decadal sea-level variability in the western Pacific, the only long-lasting tide gauge record (Fremantle) in a region of strong variability in the IO is on the west coast of Australia [*Church et al.*, 2004]. As the sea-level in this region is influenced by the western Pacific variability at both interannual and decadal timescales, the decadal sea-level pattern in the rest of the southern IO is likely to resemble the interannual pattern because of the EOF-based pattern reconstruction technique. Sea-level variations in the WO and reanalyses have no such constraint, but the decadal variability in these products is characterized by the availability of *in-situ* data (and wind forcing in reanalyses) which is poor over the 1960-2000 period in the entire southern IO (Fig. S8). The tendency of reconstructions to produce interannual-like pattern is evident even when the analysis is performed over the recent data-rich period (1980-2010 or 1993-2010, not shown). Also note that results deduced from Fig. 4 (ensemble-mean average of reconstructions vs. reanalyses) hold for individual pairs: reconstructions tend to emphasize the signal associated with decadal ENSO (and Modoki) in the southern tropical IO (Fig. S4, S5) and to reduce the amplitude of ENSO-independent signal in the south-western IO (Fig. S7) relative to the reanalyses they are derived from. Overall, the above analyses hence indicate that reconstructions may tend to accentuate ENSO-dependent signal in the IO and strongly underestimate ENSO-independent variability.

4. Discussion

Decadal sea-level variations depicted in available gridded sea-level datasets over the 1960-2010 period are generally consistent in the Pacific, with a typical standard deviation of 2-3cm. The

Pacific decadal sea-level variability is dominated by two decadal climate modes. The decadal ENSO-related basin-scale sea-level pattern in the Pacific (~50% of variance, on average) is very consistent across products and similar to that depicted by satellite altimetry over the shorter period (1993-2013). Any of these products can hence be confidently used to describe ENSO-related Pacific decadal sea-level variability. Our analysis confirms the decadal Modoki sea-level imprint (~20% of variance, on average), suggested by BY2010 based on altimetry, over a longer 50 years period. The inter-products consistency for this mode is however weaker than that related to decadal ENSO fluctuations, with consistent signals mostly in the western tropical Pacific. The time evolution of this second mode is also quite uncertain before 1980, most likely because of the limited observational coverage and larger degree of uncertainty in wind forcing.

IO decadal sea-level variations generally have a smaller amplitude (1-2 cm) than those in the Pacific and are far less consistent across the data sets. The oceanic bridge associated to ENSO between the western Pacific and west Australian coast discussed in previous studies [e.g. *Feng et al.*, 2004, 2010; *Lee and McPhaden*, 2008, N2013] is robust across products. However, the transmission of (weak) decadal Modoki sea-level signals in this region is more variable across the products. The atmospheric teleconnection between decadal ENSO and sea-level variability in the southern tropical IO, suggested by *Lee and McPhaden* [2008], appears in reconstructions but is absent in other products. The uncertainties are even larger for intrinsic (Pacific-independent) IO decadal sea-level variability. Though most of the products suggest that a large fraction of IO decadal sea-level variance is independent from the Pacific, this Pacific-independent decadal sea-level variability is highly variable across products.

This poor consistence is probably due to a data coverage that is insufficient to properly constrain IO decadal sea-level variability. There are for instance not many multi-decadal tide gauge records in the IO to constrain *reconstructions*, and in particular no records in the interior IO, while many islands host records that span several decades in the western Pacific (Fig. 1 of *Church et al.*, [2004]). On the other hand, sea level from reanalyses and WO are more dependent on *in-situ* ocean profiles that can resolve variations in upper ocean heat content. As shown in Fig. S8, while the western Pacific is being relatively well sampled since 1960, the southern IO has large gaps until the early 2000s. It is also to be noted that the IO decadal sea-level variations (the signal we are interested in) are about twice weaker than in the Pacific (Fig. 1a). On the other hand, there is a significant small-scale ‘noise’ in IO sea-level variability, for instance associated with mesoscale eddies (e.g. *Li and Han*, 2015), leading to a lower *signal-to-noise* ratio in this basin.

Most of the past literature discussing IO decadal sea-level variations largely relied on the

analysis of numerical experiments using a single model framework [e.g. *Schwarzkopf and Boning, 2011; Trenary and Han, 2013; Zhuang et al., 2013; N2013; Li and Han, 2015*]. These experiments can only be validated to the short satellite altimetry dataset or to the longer, but relatively inconsistent reanalyses and reconstructions. Except off the west Australian coast, where the different datasets are generally consistent, this can cast some doubts on the reliability of the results discussed in these studies, knowing that surface wind stress decadal variability can also significantly differ between existing products [*Nidheesh, 2017*]. It is, for instance, difficult to conclude whether there is an atmospheric teleconnection to the Pacific— possibly associated to the links between the decadal IOD and ENSO modulations – that induces a decadal sea-level response in the southern tropical IO, as suggested by *Lee and McPhaden*[2008], as this feature is only seen in reconstructions and not in reanalyses/WO. As pointed out above, the former indeed suffer from a very sparse coverage of longtide gauges in the IO while the latter are plagued by poor *in-situ* data coverage and (for reanalyses) inconsistent estimates in decadal wind variations [N2013]. It is also currently difficult to assess whether there is an intrinsic decadal sea-level variability in the IO, or its pattern, confirming the view that IOdecadal variability is a grey area [*Han et al., 2014*]. Future studies will hence be necessary to decipher whether some products can be trusted more than others, for example, by comparing these products with ocean profiles collected along multi-decadal lines of the Ship of Opportunity Program (SOOP)in key regions such as the southern and southwest tropical IO. The CMIP database also offers an interesting opportunity to investigate whether coupled models can yield a more coherent view of IO decadal variability than current observation-based sea-level datasets.

Acknowledgements

This research was funded under the “Mordicus” Agence Nationale pour la Recherche(ANR) and “SeaLevelALK” Centre National d’Etudes Spatiales (CNES) grants. The ERA4CS project ECLISEA supported the development and the production of the LEGOS sea-level reconstructions. The first five authors thank CSIR-NIO, Goa, India for providing research facilities where this study was initiated. The CW reconstruction and merged satellite altimetry are both available from CSIRO-Australia website at [https://www.cmar.csiro.au/sealevel/sl_data_cmar.html]. All the reanalyses used in this study are accessible from [<https://reanalyses.org/ocean/overview-current-reanalyses>]. The NOAA-NODC world ocean data heat content and thermosteric sea-level data are available from [<https://www.nodc.noaa.gov/access/>]. The LEGOS sea-level reconstructions are freely available at [ftp://ftp.legos.obs-mip.fr/pub/2D_sealevel_reconstruction/]. The HA sea-level reconstruction is available at: https://podaac.jpl.nasa.gov/dataset/RECON_SEA_LEVEL_OST_L4_V1.

References

- Annamalai, H., R. Murtugudde, J. Potemra, S.-P. Xie, P. Liu, and B. Wang (2003), Coupled dynamics over the IO: Spring initiation of the zonal mode, *Deep Sea Res.*, Part II, 50 (12–13), 2305–23.
- Ashok, K., S. K. Behera, S. A. Rao, H. Weng, and T. Yamagata (2007), El Niño Modoki and its possible teleconnection, *J. Geophys. Res.*, 112, C11007.
- Balmaseda, M. A., K. Mogensen, and A. T. Weaver (2013), Evaluation of the ECMWF ocean reanalysis system ORAS4, *Q. J. Roy. Meteorol. Soc.*, 139, 1132–1161.
- Behera, S. K., T. Yamagata (2010), Imprint of the El Niño Modoki on decadal sea level changes, *Geophys. Res. Lett.*, 37, L23702.
- Boyer T. P., J. I. Antonov, O. K. Baranova, H. E. Garcia, D. R. Johnson, R. A. Locarnini, A. V. Mishonov, T. D. O’Brien, D. Seidov, I. V. Smolyar, M. M. Zweng (2009), World Ocean Database 2009. S. Levitus, Ed., NOAA Atlas NESDIS 66, U.S. Gov. Printing Office, Wash., D.C., 216 pp., DVDs.
- Bromirski, P. D., A. J. Miller, R. E. Flick and G. Auad (2011), Dynamical suppression of sea level rise along the Pacific Coast of North America: Indications for imminent acceleration, *J. Geophys. Res.*, 116, C07005.
- Carton, J., B. Giese (2008), A reanalysis of ocean climate using Simple Ocean Data Assimilation (SODA), *Monthly Weather Rev.*, 136, 2999–3017.
- Church, J. A., and N. J. White (2011), Sea-level rise from the late 19th to the early 21st century, *Surv. Geophys.*, 32, 585–602.
- Church, J.A., N. J. White, R. Coleman, K. Lambeck, J.X. Mitrovica (2004), Estimates of the regional distribution of sea-level rise over the 1950 to 2000 period, *J. Clim.*, 17:2609–2625.
- Cleveland, R.B., W. S. Cleveland, J. E. McRae and I. Terpenning (1990), STL: A Seasonal-Trend Decomposition Procedure Based on Loess, *Journal of Official Statistics*, 6:3-73.
- Compo, G.P., J.S. Whitaker, P.D. Sardeshmukh, N. Matsui, R.J. Allan, X. Yin, B.E. Gleason, R.S. Vose, G. Rutledge, P. Bessemoulin, S. Brönnimann, M. Brunet, R.I. Crouthamel, A.N. Grant, P.Y. Groisman, P.D. Jones, M. Kruk, A.C. Kruger, G.J. Marshall, M. Maugeri, H.Y. Mok, Ø. Nordli, T.F. Ross, R.M. Trigo, X.L. Wang, S.D. Woodruff, and S.J. Worley (2011), The Twentieth Century Reanalysis Project, *Quarterly J. Roy. Meteorol. Soc.*, 137, 1-28. DOI: 10.1002/qj.776.
- Di Lorenzo, E., K. M. Cobb, J. C. Furtado, N. Schneider, B. T. Anderson, A. Bracco, M. A. Alexander and D. J. Vimont (2010), Central Pacific El Niño and decadal climate change in the North Pacific Ocean, *Nature Geoscience*, 3(11) 762-765.
- Dong, L., T. Zhou, A. Dai, F. Song, B. Wu, X. Chen (2016), The footprint of the inter-decadal Pacific oscillation in Indian Ocean sea surface temperatures, *Scientific reports*, 6, 21251.
- Fasullo, J.T., R. S. Nerem, B. Hamlington (2016), Is the detection of accelerated sea level rise imminent?, *Sci. Rep.*, 6, 31245.
- Feng, M., Y. Li, G. Meyers (2004), Multi-decadal variations of Fremantle sea level: Footprint of climate variability in the tropical Pacific, *Geophys. Res. Lett.*, 31:L16302.
- Feng, M., M. J. McPhaden, T. Lee (2010), Decadal variability of the Pacific subtropical cells and their influence on the southeast Indian Ocean, *Geophys. Res. Lett.*, 37:L09606.
- Feng, M., G. Meyers, A. Pearce, S. Wijffels (2003), Annual and interannual variations of the Leeuwin Current at 32°S, *J. Geophys. Res.*, 108(C11):3355.
- Frankcombe, L.M., S. McGregor, M. H. England (2015), Robustness of the Modes of Indo-Pacific Sea-level variability, *Clim Dyn.*, 45: 1281.

- Fukumori, I., R. Raghunath, L.-L. Fu (1998), Nature of global large-scale sea level variability in relation to atmospheric forcing: A modeling study, *J. Geophys. Res.*, 103(C3), 5493–5512.
- Greatbatch, R.J. (1994), A note on the representation of steric sea level in models that conserve volume rather than mass, *J. Geophys. Res.*, 99:12,767-12,771.
- Hamlington, B. D., R. R. Leben, K-Y. Kim(2012), Improving sea level reconstructions using non-sea level measurements, *J. Geophys. Res.*, 117, C10025.
- Hamlington, B. D., R. R. Leben, M. W. Strassburg, R. S. Nerem, K-Y. Kim (2013), Contribution of the Pacific Decadal Oscillation to global mean sea level trends, *Geophys. Res. Lett.*, 40: 5 171–5 175.
- Hamlington, B. D., M. W. Strassburg, R. R. Leben, W. Han, R. S. Nerem, and K.-Y. Kim (2014), Uncovering an anthropogenic sea-level rise signal in the Pacific Ocean, *Nat. Clim. Change*, 4, 782–785.
- Hamlington, B.D., R. Leben., S. Nerem, W. Han., K-Y. Kim, (2011), Reconstructing sea level using cyclostationary empirical orthogonal functions. *J. Geophys. Res.* 116, C12015.
- Han, W., J. Vialard, M. J. McPhaden, et al. (2014), Indian Ocean Decadal Variability: A Review. *Bull. Amer. Meteor. Soc.*, 95, 1679–1703.
- Kalnay, E. and co-authors (1996), The NCEP/NCAR 40-Year Reanalysis Project, *Bulletin of the American Meteorological Society*, 77(3): 437–471.
- Köhl, A., and D. Stammer(2008), Decadal sea level changes in the 50-year GECCO ocean synthesis, *Journal of Climate*, 21, 1876-1890.
- Kosaka, Y., S-P Xie (2013), Recent global-warming hiatus tied to equatorial Pacific surface cooling, *Nature*, 501, 403-407.
- Lee, S.K., W. Park, M.O. Baringer et al. (2015), Pacific origin of the abrupt increase in Indian Ocean heat content during the warming hiatus, *Nature Geoscience*, 8:445–449. doi: 10.1038/ngeo2438.
- Lee, T., and M. J. McPhaden (2008), Decadal phase change in large-scale sea level and winds in the Indo-Pacific region at the end of the 20th century, *Geophys. Res. Lett.*, 35:L01605
- Levitus, S., et al. (2012), World ocean heat content and thermosteric sea level change (0–2000 m), 1955–2010, *Geophys. Res. Lett.*, 39, L10603.
- Li, Y., W. Han (2015), Decadal sea level variations in the Indian Ocean investigated with HYCOM: Roles of climate modes, ocean internal variability, and stochastic wind forcing, *J. Clim.*, 28, 9143–9165.
- Llovel, W., and T. Lee (2015), Importance and origin of halosteric contribution to sea level change in the southeast Indian Ocean during 2005–2013, *Geophys. Res. Lett.*, 42, 1148–1157.
- Merrifield, M., (2011), A shift in western tropical Pacific sea level trends during the 1990s, *J. Climate*, 24, 4126–4138.
- Meyssignac, B., M. Becker, W. Llovel, A. Cazenave (2012a), An assessment of two-dimensional past sea level reconstructions over 1950-2009 based on tide gauge data and different input sea level grids, *Survey in Geophysics*, 33, 5:945-972.
- Meyssignac, B., D. Salas y Melia, M. Becker, W. Llovel, and A. Cazenave (2012b), Tropical Pacific spatial trend patterns in observed sea level: Internal variability and/or anthropogenic signature?, *Climate Past*, 8, 787–802.
- Moon, J.-H., Y. T. Song, P. D. Bromirski, and A. J. Miller (2013), Multi-decadal regional sea level shifts in the Pacific over 1958–2008, *J. Geophys. Res. Oceans*, 118, 7024–7035.
- Neumann, B., A. T. Vafeidis, J. Zimmermann, R. J. Nicholls (2015), Future coastal population growth and exposure to sea-level rise and coastal flooding - A global assessment, *PLoS ONE*, 10(3): e0118571, doi.org/10.1371/journal.pone.0118571.

- Newman, M., G. P. Compo, M. A. Alexander (2003), ENSO-forced variability of the Pacific decadal oscillation, *J Climate*, vol. 16, No. 23.
- Newman, M., M. Alexander, T. R. Ault, K. M. Cobb, C. Deser, E. Di Lorenzo, and co-authors (2016), The Pacific decadal oscillation, revisited, *J. Clim.*, 29, 4399–4427.
- Nidheesh, A. G., M. Lengaigne, J. Vialard, T. Izumo, A. S. Unnikrishnan and C. Cassou (2017), Influence of ENSO on the Pacific decadal oscillation in CMIP models, *Clim. Dyn.*, doi:10.1007/s00382-016-3514-8.
- Nidheesh, A. G., M. Lengaigne, J. Vialard, A. S. Unnikrishnan, and H. Dayan (2013), Decadal and long-term sea level variability in the tropical Indo-Pacific Ocean, *Climate Dyn.*, 41, 381–402.
- Nidheesh, A. G., (2017), Decadal and long-term sea-level changes in the tropical Indo-Pacific Ocean, *Ph.D.thesis*, Goa University, Goa, India.
- Nieves, V., J. K. Willis, W. C. Patzert (2015), Recent hiatus caused by decadal shift in Indo-Pacific heating, *Science*, 349(6247)532–535, 10.1126/science.aaa4521.
- Palanisamy, H., A. Cazenave, T. Delcroix, B. Meyssignac (2015), Spatial trend patterns in the Pacific Ocean sea level during the altimetry era: the contribution of thermocline depth change and internal climate variability, *Ocean Dyn.*, 65 341–56.
- Pattullo, J., W. Munk, R. Revelle, E. Strong (1955), The seasonal oscillation in sea level, *J. Mar. Res.* 14:88–156.
- Power, S., F. Tseitkin, V. Mehta, B. Lavery, S. Torok, N. Holbrook (1999), Decadal climate variability in Australia during the twentieth century, *Int. Jour. of Climatology*, vol. 19, 2, 169–184.
- Rayner, N.A., D. E. Parker, E. B. Horton et al. (2003), Global analyses of sea surface temperature, sea ice, and night marine air temperature since the late nineteenth century, *Journal of Geophysical Research, Oceans* (1978–2012), 108:4407.
- Schwarzkopf, F.U., C. W. Böning (2011), Contribution of Pacific wind stress to multi-decadal variations in upper ocean heat content and sea level in the tropical south Indian Ocean, *Geophys. Res. Lett.*, 38, L12602.
- Serazin, G. et al., (2015), Intrinsic variability of sea level from global 1/12° ocean simulations: Spatiotemporal scales, *J. Clim.*, 28, 4279–4292.
- Stammer, D., A. Cazenave, R. M. Ponte, and M. E. Tamisiea (2013), Causes for contemporary regional sea level changes, *Annual Review of Marine Science*, vol. 5, 21–46, doi:10.1146/annurev-marine-121211-172406 .
- Trenary, L., and W. Han (2013), Local and remote forcing of decadal sea level and thermocline depth variability in the south Indian Ocean, *J. Geophys. Res.*, 118, 381–398.
- Webster, P.J., A. M. Moore, J. P. Loschnigg and R. R. Leben (1999), Coupled ocean-atmospheric dynamics in the Indian Ocean during 1997-98, *Nature*, 401:356-360.
- Widlansky, M. J., A. Timmermann, and W. Cai, (2015), Future extreme sea level seesaws in the tropical Pacific, *Sci. Adv.*, 1, e1500560, doi:10.1126/sciadv.1500560.
- Woodworth, P. L., R. Player (2003), The Permanent Service for Mean Sea Level: an update to the 21st century, *Journal of Coastal Research*, 19:287-295.
- Zhang, X., and J. A. Church (2012), Sea level trends, interannual and decadal variability in the Pacific Ocean, *Geophys. Res. Lett.*, 39, L21701.
- Zhuang, W., M. Feng, Y. Du, A. Schiller, and D. Wang (2013), Low-frequency sea level variability in the southern Indian Ocean and its impacts on the oceanic meridional transports, *J. Geophys. Res.*, 118, 1302–1315.

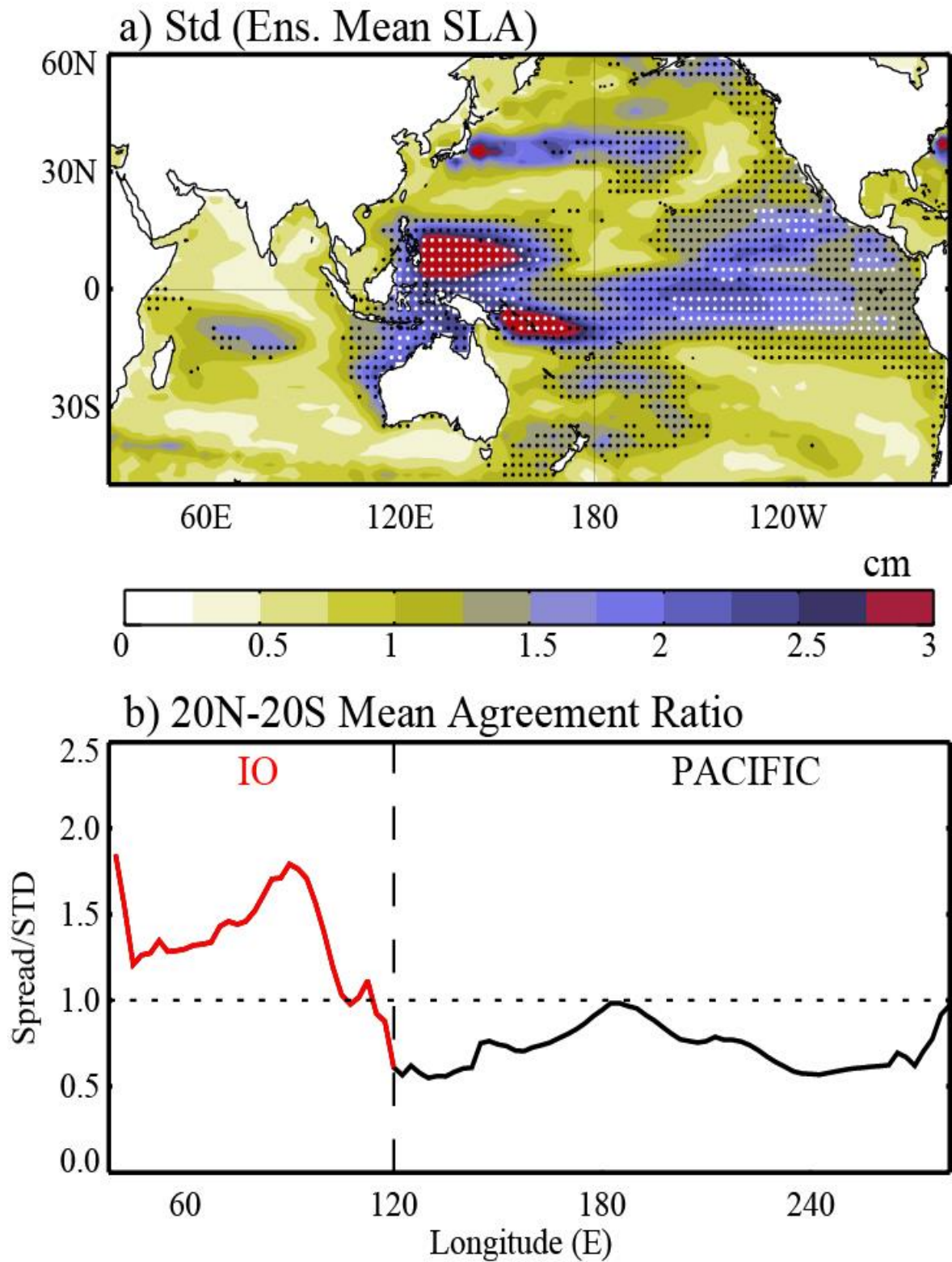


Figure 1: (a) Standard deviation (Std) of the ensemble-mean decadal sea-level variability from the ten gridded products analyzed (color). Black (resp. white) dots indicate regions where the “agreement ratio” is below 1 (resp. 0.5). A small agreement ratio means that the differences in variability between the products (spread) are small relative to the mean amplitude of variability (Std) (see *Data and method* section and supplementary material for details). (b) Zonal distribution of the 20°N-20°S averaged agreement ratio in the Indo-Pacific.

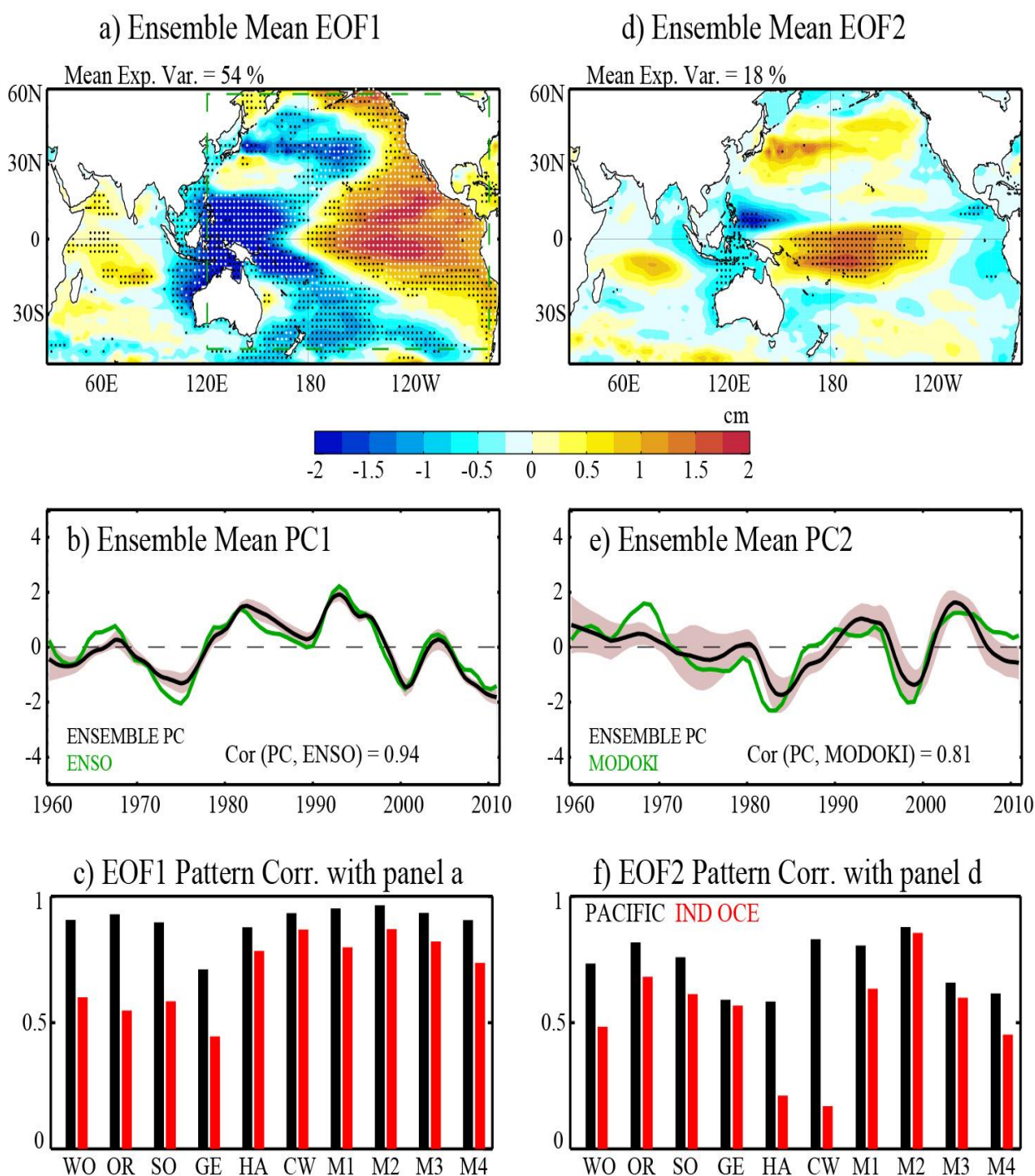


Figure 2: Ensemble mean of the (a) first and (d) second EOF of Pacific decadal sea-level variations across the ten analyzed gridded products (color). The EOFs are computed over the domain highlighted by the green frame in panel a (with a mask to discard western Atlantic). The pattern outside the EOF domain is obtained by linearly regressing the decadal sea-level anomalies onto the corresponding normalized principal component (PC) for each product. As in Figure 1a, black (white) dots indicate regions where the spread amongst the products is smaller (twice smaller) than the mean amplitude associated with that EOF (see supplementary material for details). (b, e) Corresponding ensemble mean PCs (black curves) with the shading indicating \pm one standard deviation. Decadal ENSO and Modoki indices are displayed by the green curves on panels b and e respectively. (c, f) Bar diagram showing the Pacific (black) and IO (red) pattern correlation between the EOF pattern for individual product and the ensemble mean EOF pattern shown on panel a and d.

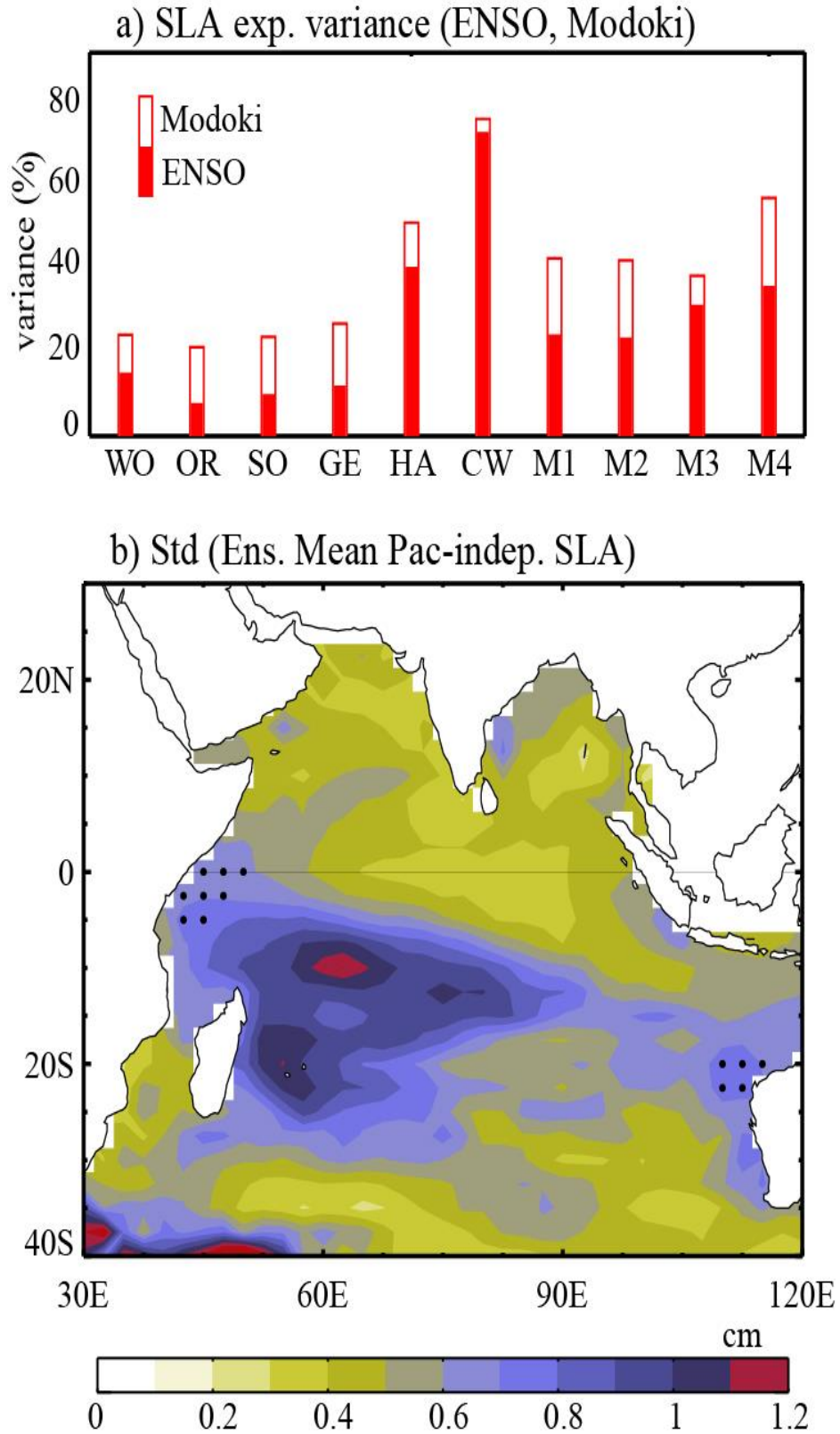


Figure 3: (a) Bar diagram showing the respective contribution of decadal ENSO (filled red bar) and Modoki (unfilled) to the total decadal sea-level variance in the IO for each data. (b) Standard deviation of the ensemble mean decadal sea-level variability in the IO, once the variability associated with decadal ENSO and Modoki is removed through a multi-linear regression. A similar stippling as on Figure 1a is applied on panel b to indicate the regions where this Pacific-independent variability across the products is robust.

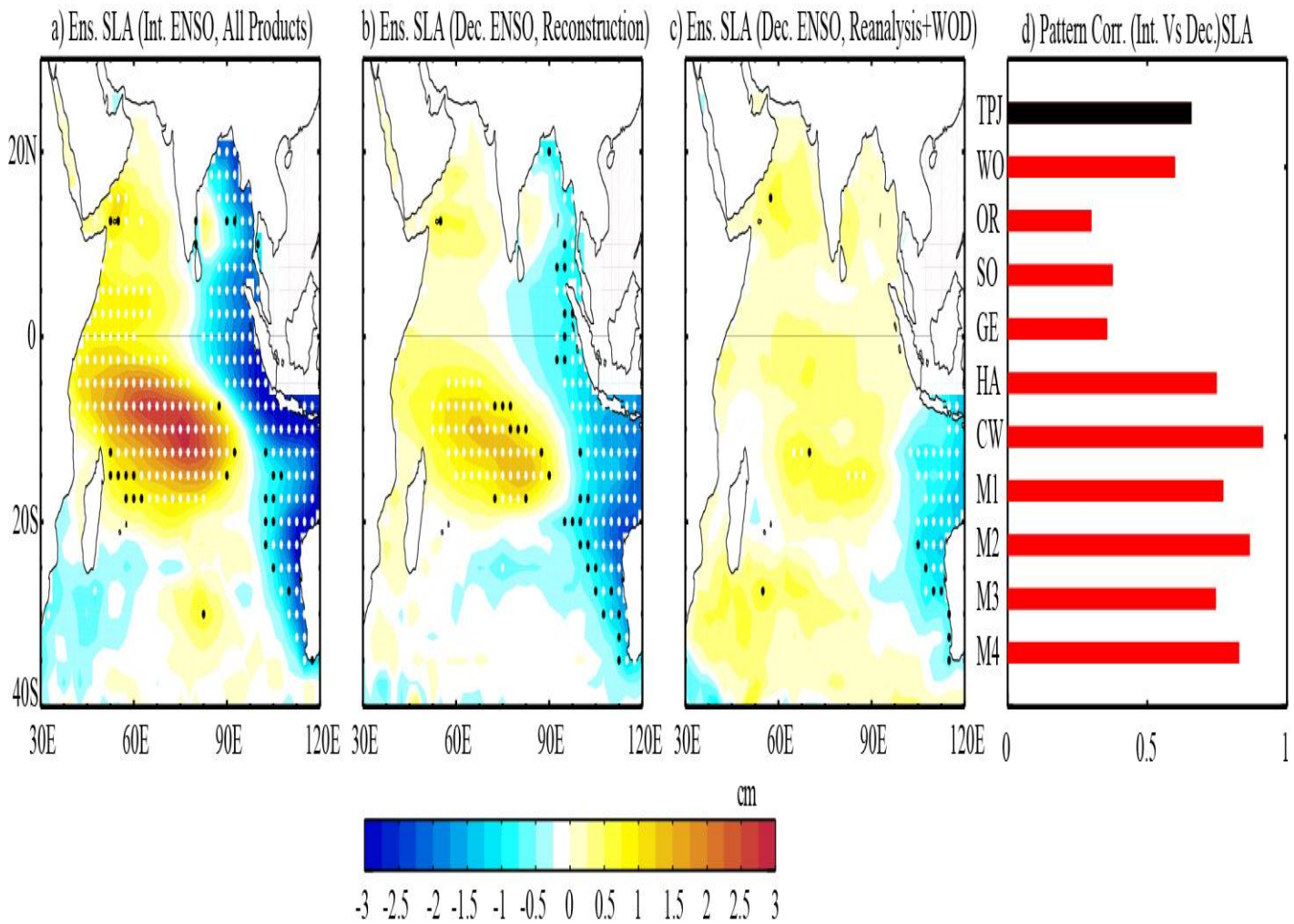


Figure 4: (a) Ensemble mean of IO sea-level anomalies (SLA) linearly related to interannual ENSO index for the ten analyzed gridded products. Ensemble mean of IO SLA linearly related to decadal ENSO for (b) the six sea-level reconstructions and (c) the three ocean reanalyses and WO. (d) Pattern correlation between the IO SLA associated with interannual and decadal ENSO for each product. A high correlation indicates that the interannual and decadal ENSO signatures have similar patterns in the IO for a given product.